International Journal of Engineering & Technology, 7 (3.19) (2018) 113-118

International Journal of Engineering & Technology

Website: www.sciencepubco.com/index.php/IJET

Research paper

Some Factors Affecting on Magnetic Characteristic Quantities and T_c Curie Phase Transition Temperature of the Ni Nanoparticles by the Classical Heisenberg Model

Nguyen Trong Dung[1,*] , Pham Khac Hung[2]

[1,*] Faculty of Physics, Hanoi National University of Education, Vietnam
[2] School of Engineering Physics, Hanoi University of Science and Technology, Vietnam
Email address: [1] dungntsphn@gmail.com, [2] pkhung@fpt.vn

Abstract

This paper investigates the effect of particle size D = 4.51nm, 5.03nm, 5.42nm, 5.91nm, rate of heat 4.10^{12}K/s, 4.10^{13}K/s, 4.10^{14}K/s on magnetic characteristic quantities: Magnetization M, specific heat Cv, energy E, magnetic susceptibility χ and T_c Curie phase transition temperature by classical Heisenberg model. The results show when increasing D particle size then T_c Curie transition temperature increases and when increasing rate of heat then T_c decreasing. In addition, there is the influence of D size and heating rate on magnetic characteristic quantities.

Keywords: *influence, particle size, rate of heat, T_c Curie transition temperature, classical Heisenberg model.*

1. Introduction

Now, Ni nanomaterials are being used in the science, technology and biomedical. Optical catalysts [1], [2], photovoltaics [11], solar cells [3], [4]. .. To create the Ni nanoparticles, there are many methods. Chemical methods [5], [6], [7], physical methods [8], [9] ... and molecular dynamics simulation methods [30] and Monte-Carlo method [31]. The results showed, T_m phase transition temperature always proportional with $N^{-1/3}$ atoms number [10], [11], [12], [13], [14], [15], T_g crystallization temperature of the nanowires always inversely proportional with D size [11] and T_c Curie phase temperature be determined by semi-empirical formula give results smaller than 631K [16]. For size D = 24nm, 50nm, 96nm, 165nm, 200nm then T_c = 593K, 612K, 622K, 626K, 627K and when D decreases then T_c decreases [17], [18], [19], [20], [21], [22], [23], [24], [25], [26], [27], [28], [29]. In addition, there is also the effect of Ni nanoparticle size [49] and thin film thickness [50] on T_c Curie transition temperature. Recently, investigated the effect of rate of heat, atomic number, temperature, and heating time on structure of Ni nanoparticles by Molecular Dynamics method with Sutton-Chen interaction, boundary conditions freedom [30] and characteristic quantities magnetic of Fe nanoparticles [31]. The results show, has influence of D particle size on structure and magnetism. When increasing atomic number N lead to D particle size increases proportional with $N^{-1/3}$ and energy increases proportional with N^{-1} [30] and appearance of BCC structure is interesting and controversial. With calculations based on analysis: Structural [45], [47] link angle analysis [46], link analysis [48] ... will solve this problem, T_c Curie phase temperature increased [31]. In the article, influence of D particle size, rate of heat on magnetic characteristic quantities and T_c Curie phase transition temperature of Ni nanoparticles.

2. Calculation Method

The study Ni nanoparticle with density ρ and nanoparticle size evaluated by $D = 2\left(\frac{3N}{4\pi\rho}\right)^{1/3}$ (1)

with ρ = 7.72 g.cm^{-3}. Inside N, V are atoms numbers total and volume of particle. Ni nanoparticles generated by molecular dynamics method with embedded interaction Sutton-Chen and free boundary condition [30]. The thermal processes follow law of Nosé el [43] and Hoover el [44]. To determine magnetic characteristic properties, considered each atom of Ni nanoparticle is an spin S_i, magnitude value of each spin is $|S_i|$ = 1. Place Ni nanoparticles into classical Heisenberg model [32], [33], [34] with Hamilton function has form:

$$H=-\sum_{r_{ij}\hat{I}R_{(i)}} J_{ij}\left(r_{ij}\right)\left(S_i \times S_j\right) \quad (2)$$

$$\text{In it } J_{ij}\left(r_{ij}\right)=J_0\left(1-\frac{\left|r_{ij}\right|}{r_c}\right)^3 \quad (3)$$

With J_0 is interaction energy between two nearest spins, $r_{ij}=\left|r_i-r_j\right|$ is shortest distance between two spins S_i, S_j and J_{ij} is interaction energy between spins S_i, S_j and r_c = 3.35Å is radius breaker. After that determining magnetic characteristics of nanoparticles Ni as:

$$\langle E\rangle=\frac{1}{N}\langle H\rangle,\langle M\rangle=\frac{1}{N}\left\langle\left|\sum_i S_i\right|\right\rangle,$$
$$\langle C_v\rangle=N\frac{\langle E^2\rangle-\langle E\rangle^2}{(k_BT)^2},\langle\chi\rangle=N\frac{\langle M^2\rangle-\langle M\rangle^2}{k_BT} \quad (4)$$

and T_c Curie phase transition temperature.

Inside, magnetic characteristic quantities has related to J_0 interaction energy which is currently unknown by theory model well as in empirical. used Moten-Carlo method, combined with error method of physical quantity measurement to determine J_0 by:

First, determining average value of $\overline{T}_c = \frac{1}{N}\sum_{i=1}^{N} T_c$ and absolute error $\Delta T_c = \left|T_c - \overline{T}_c\right|$ of Ni_{4000} nanoparticles with D = 4.51nm according J_0 = 0.4; 0.5; 0.6; 0.61; 0.63; 0.65; 0.67; 0.69; 0.7; 0.8 and comparing obtained results T_c with results of semi-empirical formula T_{es} (5) and then selecting J_0 with minimum ΔT_c absolute error.

$$T_{es}(D) = T_{c0}\exp\left(-\frac{2S_{vib}}{3R}\frac{1}{D/6h-1}\right) \quad (5)$$

With $S_b \approx S_m$ = 10,12 J/mol.K; h = 0,2492nm; T_{c0} = 631K; R = 8,314 J/mol.K [35], [36], [37] have T_{es} of Ni nanomaterials. All of the nanoparticles were done with sufficient time to reduce statistical errors. Recovery time is 10^6 MC steps/spin and the average statistical time is 2.10^6 MC steps/spin.

3. Results and Discussion

3.1. Effect of J_0 Exchange Energy

To determine T_c Curie phase transition temperature of Ni_{4000} nanoparticle [30] with different J_0 exchange energy values, resulting Table 1, Figureure. 1

Table 1 Relationship between T_c Curie phase transition temperature with J_0 exchange energy of Ni_{4000} nanoparticles

J_0	T_c(K)	$\overline{T}_c(K)$	$\Delta T_c = \left\|T_c - \overline{T}_c\right\|(K)$
J_0 = 0.4	271.6		131.7
J_0 = 0.5	339.5	403.3	63.8
J_0 = 0.6	400.6		2.71
J_0 = 0.7	468.6		65.3
J_0 = 0.8	536.4		133.1

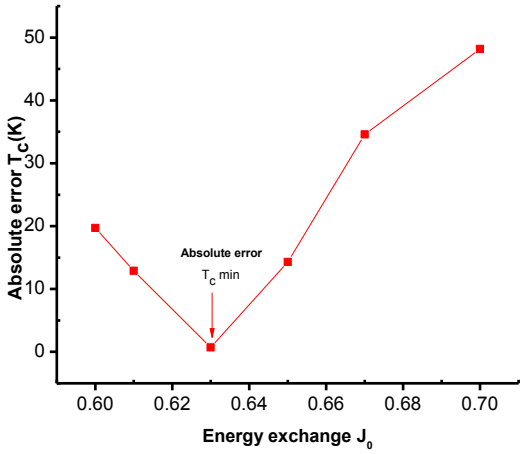

Figureure 1 The relationship between the absolute error of T_c curie phase transition temperature with J_0 exchange energy values differently.

The results show, T_c Curie phase transition temperature has average value $\overline{T}_c$ = 403.3K (table 1) and in range J_0 = (0.6; 0.7). The detailed result shows J_0 = 0.63 a has smallest absolute error (Figureure 1). So, choose J_0 = 0.63, with neighborhood radius r_c = 3.35Å to study. This is method very useful for theory studies, empirical to determine J_0 values for a variety of materials.

3.2. Effect of D Particle Size

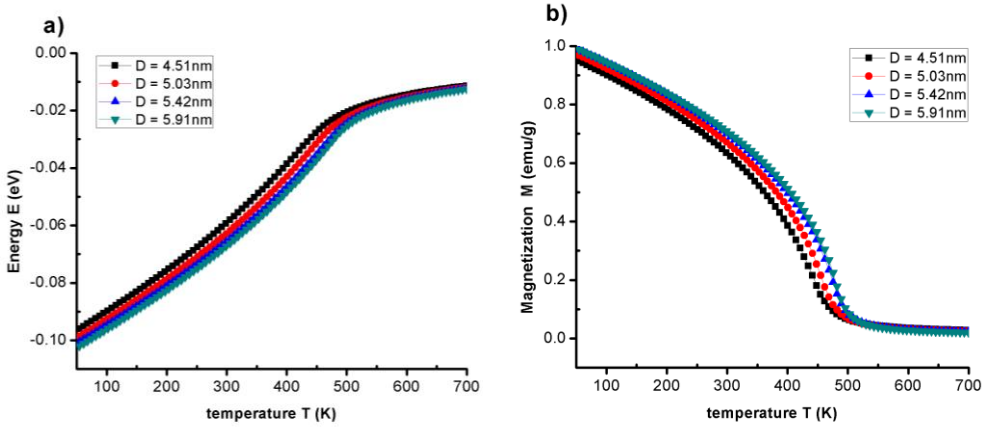

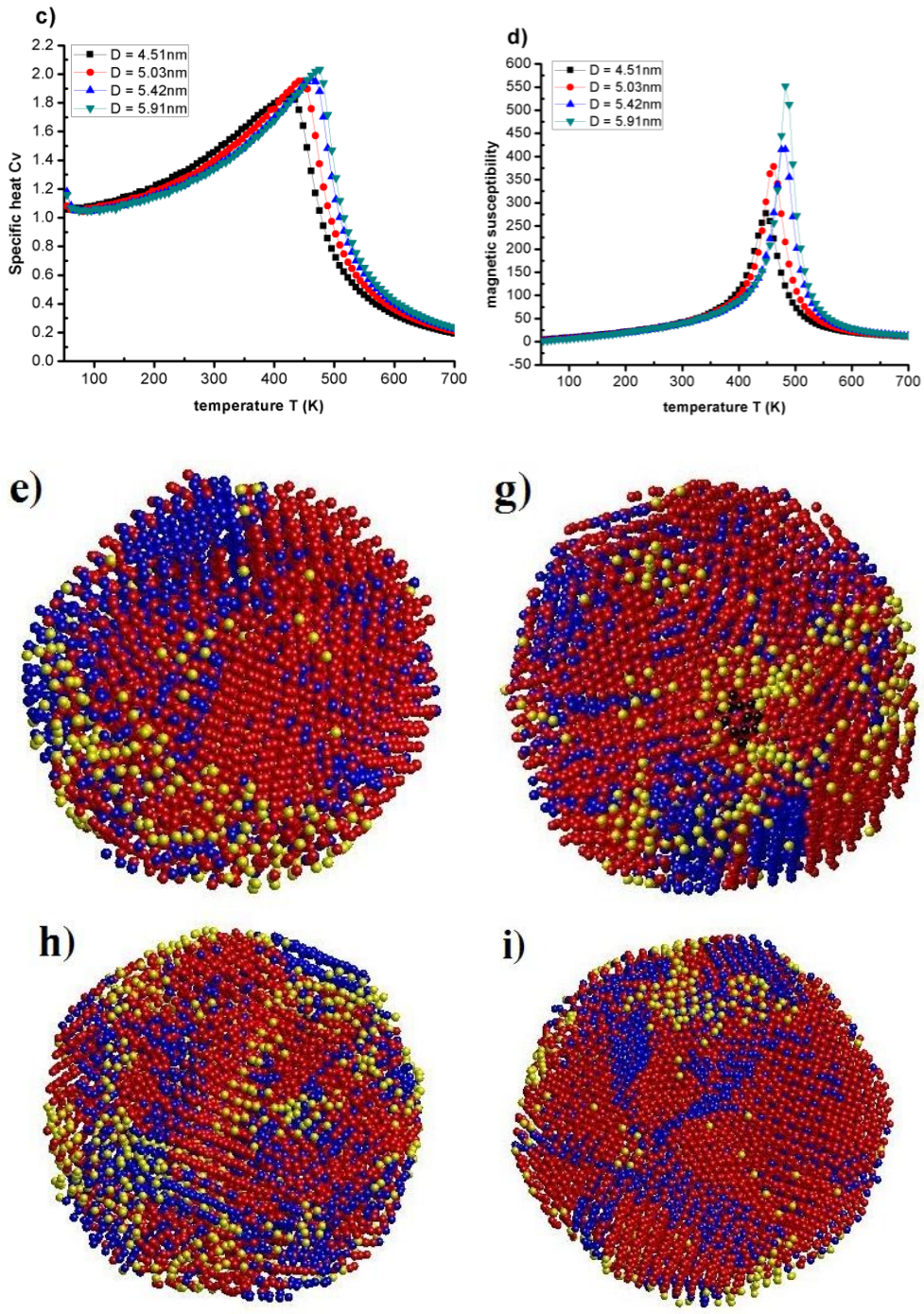

Figureure 2. E Energy (Fig. a), M magnetization (Fig. b), Cv specific heat (Fig. c), χ magnetic susceptibility (Fig. d) with D different nanoparticle size: D = 4.51nm (Fig. e), D = 5.03nm (Fig. g), D = 5.42nm (Fig. h) and D = 5.91nm (Fig. i). Inside, atoms illustrat by Red colored for FCC structure, blue for HCP structure, black for BCC structure, yellow for Amor structure.

The results show, the have influence of D on E, M, C_v, χ. When D increases from D = 4.51nm to 5.91nm then E decreases from -0.0972eV to -0.1003eV (Fig. 2a); M decreases from 1 to 0 and curvature descending (Fig. 2b); C_v reached extreme value at T_c, height of peak increased from 1.79257 to 2.0118 (Fig. 2c); height of peak increased from 276.59 to 550.83 (Fig. 2d). The displays for each T values correspond to a value M, C_v, E, in particular. The display values do not include errors because error value at point each has less than size of display value. When $T < T_c$ then the curvature of the magnetization curve M increases when increasing D (Fig. 2b), decreasing when $T > T_c$ and this is the basis for existence ferromagnetic phase transition on Ni nanoparticles.

In addition, the results of Fig. 2c, Fig. 2d show that extreme values of C_v and χ increase when D increases and confirmed that Tc Curie phase transition temperature of Ni nanoparticles is phase transition temperature of type 1. To the observe structure of Ni nanoparticles, used the visualization method (Fig. 2e-2i). The results show, nanoparticles are made up of FCC, HCP, BCC, Amor structures and assert there is no messy arrangement of Ni atoms but instead is an arrangement of atoms according to the definite structure. In Ni_{5324} nanoparticle has the appearance of BCC structure, explained in the article [30]. When increase N atoms number leading to D increase and E decreases it shows has the influence of D nanoparticle size on Ni nanoparticle structure.

To confirm the accuracy of results, compared results T_c simulation with results of semi-empirical formula T_{es} (5) [28], [29], [36], results in Table 2, Figureure 3.

Table 2. Comparison T_c Curie phase transition temperature of simulation method and T_{es} Curie phase transition temperature of semi-empirical with D different nanoparticle size.

N Number (atoms) D Size (nm)	**4000** 4.51	**5324** 5.03	**6912** 5.42	**8788** 5.91
T_c(K) (simulation)	421 ± 3	448 ± 2	461 ± 4	475 ± 6
T_{es}(K) (semi-experimental formula) [28], [29], [36]	422	448	463	479

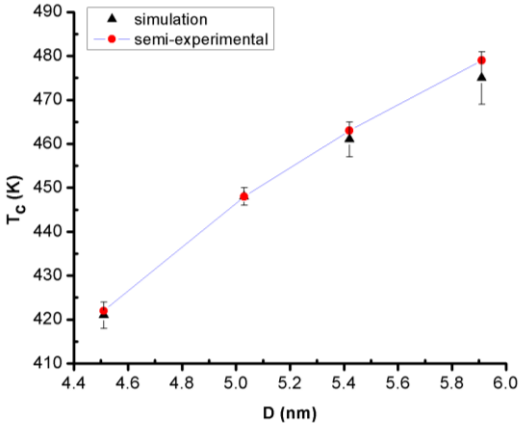

Figureure 3. The relationship between T_c Curie phase transition temperature of simulation method and T_{es} Curie phase transition temperature results of semi-empirical formula with D nanoparticles sizes differently.

The results show, with each value of D will have T_c value, T_{es} respectively. To evaluate error at each value T_c and T_{es} use the interpolation method. These results showed, table 2 including T_c value respectively, error value at each point and T_{es} is determined by semi-empirical formula (5) to the comparison. Here determined the relationship between T_c and T_{es}: $T_{es} = T_c \pm (2 \text{ or } 6)$ K with D increased from 4.51 nm to 5.91 nm. After comparing results between T_c and T_{es} [28], [29], [36] (Fig. 3) show results has duplication. The simulated results show that it is not only consistent with results of semi-empirical formula but also good fit with simulation results of bulk material and thin films [29], [38], [39], [41], [42], [49], [50] the value obtained within allowable limit and confirmed by influence of D on magnetic characteristic quantities and T_c.

3.3 Effect of Heating Rate

To study magnetic characteristics and T_c Curie phase transition temperature at different structural states corresponding with different heating rates results in Figureure 4

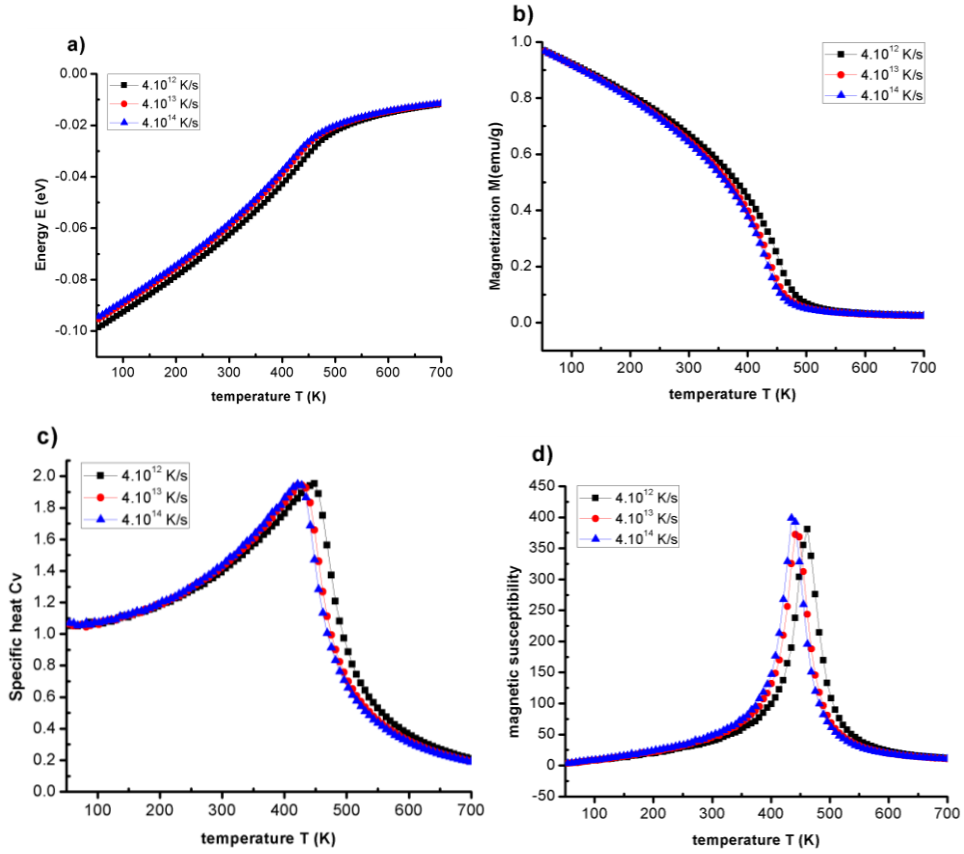

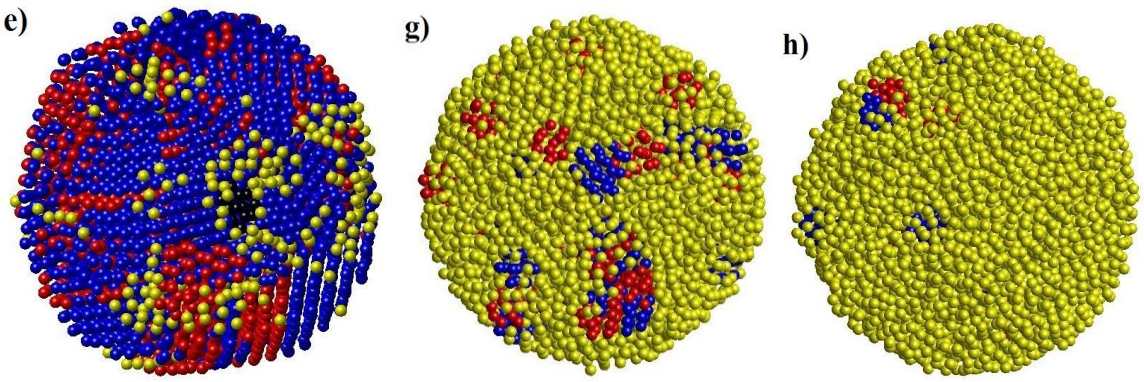

Figureure 4 Magnetic characteristics of Ni_{5324} nanoparticles: Energy (Fig. a), magnetization (Fig. b), specific heat (Fig. c), magnetic susceptibility (Fig. d) with different heating rates 4.10^{13}K/s (Fig. e), 4.10^{13}K/s (Fig. g), 4.10^{14}K/s (Fig. h) at temperature of T = 300K.

The results show, when increased rates of heating from 4.10^{12}K/s to 4.10^{14}K/s then energy increased (Fig. 4a), magnetization decreases (Fig. 4b), specific heat is constant (Fig. 4c) while magnetic susceptibility change negligible (Fig. 4d). When heating rate increases lead to T_c Curie phase transition temperatures decreases it shows Ni nanoparticles have moved on the amorphous state. Results structural change from crystalline state to the amorphous state leading to energy increased. The structural shape results (Fig. 4e-4h) shown HCP, FCC structural unit number decrease, and Amor increase is 93.98%. These results are consistent with results shown in Figureure 4a-4d and very useful for studying structure and magnetism of Ni nanoparticles.

4. Conclusion

Study on effect of particle size, the heating rate on magnetic characteristic and Curie T_c phase transition temperature of Ni nanoparticles, results obtained: Successful determination of nanoparticle exchange energy is 0.63. When nanoparticle size increased lead to T_c Curie phase transition temperature increased, results were consistent with article [28], [29], [36]. When heating rate increases lead to structure changes from crystalline state to the amorphous state resulting T_c decrease. This is due to the structural change from crystalline state to the amorphous state leading to energy increased. The simulated results show it is not only consistent with the results of the semi-empirical formula but also consistent with results of bulk material and thin films [29], [38], [39], [41], [42]], [49], [50].

Acknowledgement

Thank Associate Professor Associate Professor V. Thanh Ngo for helpful comments and suggestions.

References

[1] Wang, H. Yin, M. Ren, H. Lu, J. Xue and T. Jiang, (2010), "Preparation of nickel nanoparticles with different sizes and structures and catalytic activity in the hydrogenation of p-nitrophenol", New J. Chem., 34, 708–713.
[2] Y. G. Morozov, O. V. Belousova and M. V. Kuznetsov, (2011), "Electric field-assisted levitation-jet aerosol synthesis of Ni/NiO nanoparticles", Inorg, Mater., 47, 36–40
[3] Y. Ruan, C. Wang and J. Jiang, (2016), "Nanostructured Ni compounds as electrode materials towards high-performance electrochemical capacitors", J. Mater. Chem. A, 4, 14509–14538.
[4] L. Gaouyat, Z. He, J.-F. Colomer, D. Schryvers, F. Mirabella and O. Deparis, (2015), "in Linking Optical: Properties and Nanostructure of NiCrOx Cermet Nanocomposite for Solar Thermal Application ", Springer Netherlands, Nano-Structures for Optics and Photonics, pp 497-497
[5] H. Schmidt, (2001), "Nanoparticles by chemical synthesis, processing to materials and innovative applications", Appl. Organomet. Chem., 15, 331–343.
[6] K.-C. Huang and S. H. Ehrman, (2007), "Synthesis of Iron Nanoparticles via Chemical Reduction with Palladium Ion Seeds", Langmuir, 23, 1419–1426.
[7] D. V. Goia, J. Mater, (2004), "Preparation and formation mechanisms of uniform metallic particles in homogeneous solutions", Chem., 14, 451–458.
[8] N. S. Tabrizi, Q. Xu, N. M. van der Pers, U. Lafont and A. Schmidt-Ott, (2009), "Synthesis of mixed metallic nanoparticles by spark discharge", J. Nanopart. Res., 11, 1209.
[9] H. F¨ roster, C. Wolfrum and W. Peukert, (2012), "Experimental study of metal nanoparticle synthesis by an arc evaporation / condensation process", J. Nanopart. Res., 14, 926.
[10] Y. Qi, T. Ça˘gin, W. L. Johnson and W. A. Goddard III, (2001), "Melting and crystallization in Ni nanoclusters: The mesoscale regime", The Journal of Chemical Physics 115, PP 385-394.
[11] Y.-H. Wen, Z.-Z. Zhu, R. Zhu and G.-F. Shao, (2004), "Size effects on the melting of nickel nanowires: a molecular dynamics study", Physica E: Low-dimensional Systems and Nanostructures, 25, pp 47 – 54.
[12] Y. Zhang, L. Wang and W. Wang, (2007), "Thermodynamic, dynamic and structural relaxation in supercooled liquid and glassy Ni below the critical temperature", J. Phys.: Cond. Matt., 19, 196106.
[13] L. Kelchner, S. J. Plimpton and J. C. Hamilton, (1998), "Dislocation nucleation and defect structure during surface indentation", Phys. Rev. B, 58, pp 11085–11088.
[14] 14. A. N. Andriotis, Z. G. Fthenakis and M. Menon, (2007), "Correlated variation of melting and Curie temperatures of nickel clusters", Phys. Rev. B, 75, 073413.
[15] 15. C. S. Tian, D. Qian, D. Wu, et, (2005), "Body-Centered-Cubic Ni and Its Magnetic Properties", Phys. Rev. Lett., 94, 137210.
[16] 16. X. He, H. Shi, (2012), "Size and shape effects on magnetic properties of Ni nanoparticles", Particuology 10 (4), pp 497–502.
[17] 17. C. Q. Sun, W. H. Zhong, S. Li, B. K. Tay, H. L. Bai, E. Y. Jiang, (2004), "Coordination imperfection suppressed phase stability of ferromagnetic, ferroelectric, and superconductive nano solids", The Journal of Physical Chemistry 235 B 108 (3), pp 1080–1084.
[18] 18. A. Zaim, M. Kerouad, M. Boughrara, (2013), "Monte Carlo study of the magnetic behavior of a mixed spin (1, 3/2) ferrimagnetic nanoparticle", Solid State Communications 158, 76–81.
[19] 19. C. Saikia, A. Hussain, A. Ramteke, H. K. Sharma, T. K. Maji, (2014), "Carboxymethyl starch-chitosan-coated iron oxide magnetic nanoparticles for controlled delivery of isoniazid", Journal of Microencapsulation 32 (1), pp 29–39. doi:10.3109/02652048.2014.940015. 13
[20] 20. D. Caruntu, G. Caruntu, C. J. O'Connor, (2007) "Magnetic properties of variable-sized Fe3O4 nanoparticles synthesized from non-aqueous homogeneous solutions of polyols", Journal of Physics D: Applied Physics 40 (19), pp5801–5809.
[21] 21. G. F. Goya, T. S. Berqu´o, F. C. Fonseca, M. P. Morales, (2003), "Static and dynamic magnetic properties of spherical magnetite nanoparticles", Journal of Applied Physics 94 (5), pp 3520–3528.

[22] 22. M. Jeun, S. Lee, J. K. Kang, A. Tomitaka, K. W. Kang, Y. I. Kim, Y. Takemura, K.-W. Chung, J. Kwak, S. Bae, (2012), "Physical limits of pure superparamagnetic Fe3O4 nanoparticles for a local hyperthermia agent in nanomedicine", Applied Physics Letters 100 (9), 092406.
[23] 23. Q. Jiang, X. Cui, M. Zhao, (2004), "Size effects on curie temperature of ferroelectric particles", Applied Physics A: Materials Science & Processing 78 (5), pp 703–704.
[24] 24. Z. Huang, Z. Chen, S. Li, Q. Feng, F. Zhang, Y. Du, (2006), "Effects of size and surface anisotropy on thermal magnetization and hysteresis in the magnetic clusters", The European Physical Journal B 51 (1), pp 65–73.
[25] 25. Xuehong Liao, Junjie Zhu, Wei Zhong, Hong-Yuan Chen, (2001), "Synthesis of amorphous Fe2O3 nanoparticles by microwave irradiation", Materials Letters, Vol 50, Issues 5–6, pp 341-346.
[26] 26. K. Ishikawa, K. Yoshikawa, N. Okada, (1988), "Size effect on the ferroelectric phase transition in PbTiO3 ultrafine particles", Physical Review B 37 (10), 5852–5855.
[27] 27. W. L. Zhong, B. Jiang, P. L. Zhang, J. M. Ma, H. M. Cheng, Z. H. Yang, (1993) "Phase transition in PbTiO3 ultrafine particles of different sizes", Journal of Physics: Condensed Matter 5 (16), pp 2619–2624.
[28] 28. X. He, H. Shi, (2012), "Size and shape effects on magnetic properties of Ni nanoparticles", Particuology 10 (4), pp 497–502.
[29] 29. H. M. Lu, W. T. Zheng, Q. Jiang, (2007), "Saturation magnetization of ferromagnetic and ferrimagnetic nanocrystals at room temperature", Journal of Physics D: Applied Physics 40 (2), pp 320–325.
[30] 30. Trong Dung Nguyen, Chinh Cuong Nguyen and Vinh Hung Tran, (2017), "Molecular dynamics study of microscopic structures, phase transitions and dynamic crystallization in Ni nanoparticles", RSC Adv, 7, 25406.
[31] 31. Trong Dung Nguyen, Chinh Cuong Nguyen, The Toan Nguyen, Khac Hung Pham, (2018), "Factors on the magnetic properties of the iron nanoparticles by classical Heisenberg model", Physica B 532 144–148.
[32] 32. C. P. Chui and Yan Zhou, (2014), "Investigating the magneto volume effect in isotropic body-centered-cubic iron using spin-lattice dynamics simulations", Aip advances 4, pp. 087123/10
[33] 33. P. W. Ma, S. L. Dudarev, A. A. Semenov and C. H. Woo, (2010), "Temperature for a dynamic spin ensemble", Phys Rev E 82, pp. 031111/6
[34] 34. P.-W. Ma, C. H. Woo, and S. L. Dudarev, (2008), "Large-scale simulation of the spin-lattice dynamics in ferromagnetic iron", Phys. Rev. B 78, pp. 024434/12
[35] 35. Ahmed Zaim and Mohamed Kerouad, (2010), "Monte Carlo study of the possibility of two compensation points in a ferrimagnetic core/shell nanoparticle Ising model" M. J. Condensed Matter. Vol. 12, number 2, pp. 77-80
[36] 36. C. Yang, Q. Jiang, (2005), "Size and interface effects on critical temperatures of ferromagnetic, ferroelectric and superconductive nanocrystals", Acta Mate-Aurilia 53 (11), 3305–3311.
[37] 37. Jiang, Q., Zhao, D. S., & Zhao, M, (2001), "Size-dependent interface energy and related interface stress". Acta Materialia, 49, pp 3143–3147.
[38] 38. H. Wang, Y. Zhou, D. Lin, C. Wang, (2002), "Phase diagram of ising nano- particles with cubic structures", Physica Status Solidi (b) 232 (2), pp 254–263.
[39] 39. P.-W. Ma, C. Woo, S. Dudarev, (2009), "High-temperature dynamics of surface magnetism in iron thin films", Philosophical Magazine 89 (32), 2921– 2933.
[40] 40. Q. Jiang, D. Zhao, M. Zhao, (2001), "Size-dependent interface energy and related interface stress", Acta Materialia 49 (16), pp 3143–3147.
[41] 41. RC Weast, MJ Astle, WH Beyer, (1989), "CRC Handbook of Chemistry and Physics", 69th Edition, CRC Press., Inc.,.
[42] 42. V. T. Ngo, H. T. Diep, (2007), "Effects of frustrated surface in heisenberg thin films", Physical Review B 75, 035412,
[43] 43. S. Nos´ e, (1984), "A unified formulation of the constant temperature molecular dynamics methods", J. Chem. Phys., 81, pp. 511–519.
[44] 44. W. G. Hoover, (1985), "Canonical dynamics: Equilibrium phase-space distributions", Phys. Rev. A, 31, pp. 1695–1697.
[45] 45. C. L. Kelchner, S. J. Plimpton and J. C. Hamilton, (1998), " Dislocation nucleation and defect structure during surface indentation", Phys. Rev. B, 58, pp 11085–11088.
[46] 46. G. J. Ackland and A. P. Jones, (2006), "Applications of local crystal structure measures in experiment and simulation", Phys. Rev. B, 73, pp. 054104/7.
[47] 47. J. Li, (2003), "AtomEye: an efficient atomistic configuration viewer", Model Simul Mater Sci Eng, 11, pp. 173-177.
[48] 48. P. J. Steinhardt, D. R. Nelson and M. Ronchetti, (1983), "Bond-orientational order in liquids and glasses", Phys. Rev. B, 28, pp. 784–805.
[49] 49. H. Amekura, Y. Fudamoto, Y. Takeda, and N. Kishimoto, (2005), "Curie transition of superparamagnetic nickel nanoparticles in silica glass: A phase transition in a finite size system", Physical Review B 71, 172404.
[50] 50. Aitor F. Lopeandía, F. Pi, and J. Rodríguez-Viejo, (2008), "Nanocalorimetric analysis of the ferromagnetic transition in ultrathin films of nickel", Applied Physics Letters 92, 122503.